

**COMPUTATIONAL STUDIES ON MUONIATED
ACETOPHENONES**

NUR AISYAH BINTI MOHAMAD ROSLI

UNIVERSITI SAINS MALAYSIA

2020

COMPUTATIONAL STUDIES ON MUONIATED ACETOPHENONES

by

NUR AISYAH BINTI MOHAMAD ROSLI

**Thesis submitted in fulfillment of the requirements
for the Degree of
Master of Sciences**

October 2020

ACKNOWLEDGEMENT

I would like to express my gratitude first and foremost to my supervisors Associate Professor Dr Mohamed Ismail Mohamed Ibrahim and Professor Dr. Shukri Sulaiman for providing me with the most appreciated guidance, advice and support to complete my study. For my laboratory mates in the Computational Chemistry and Physics Laboratory, thank you so much. I greatly appreciate all the kindness, assistance and support from all of you. Besides that, I am very grateful to my mother, brothers and sister for their support and encouragement for me to finish my master degree. It is also an honour to convey my thankfulness to the Ministry of Higher Education for providing me MyBrain 15 scholarship for this study. Above all, to the Great Almighty, the author of knowledge and wisdom, for the countless love.

TABLE OF CONTENTS

ACKNOWLEDGEMENT	ii
TABLE OF CONTENTS	iii
LIST OF TABLES	vi
LIST OF FIGURES	viii
LIST OF SYMBOLS	x
LIST OF ABBREVIATIONS	xi
LIST OF APPENDICES	xii
ABSTRAK	xiii
ABSTRACT	xv
CHAPTER 1 INTRODUCTION	1
1.1 Research Background.....	1
1.2 Problem Statement	2
1.3 Objectives.....	3
1.4 Scope of Study	3
CHAPTER 2 LITERATURE REVIEW	7
2.1 Muon and Muonium.....	7
2.2 Introduction to μ SR Techniques	9
2.3 Acetophenones	10
2.4 Related Studies on Muoniated Systems	13
CHAPTER 3 METHODOLOGY	17
3.1 Computational Study.....	17
3.1.1 Molecular Mechanics	18
3.1.2 Electronic Structure Methods.....	19
3.2 <i>Ab initio</i> Methods.....	19
3.2.1 Hartree-Fock (HF).....	20

3.2.2	Density Functional Theory (DFT)	21
3.3	Theoretical Background	22
3.3.1	The Schrödinger Equation.....	22
3.3.2	The Born-Oppenheimer Approximation	23
3.4	Muonium Hyperfine Interaction	24
3.5	Softwares.....	26
3.5.1	Gaussian09 Program	26
3.5.2	Gauss View 5.0	26
3.5.3	Basis Set	27
3.6	Pure System of Substituted Acetophenone	29
3.7	Muoniated Substituted Acetophenone	30
3.8	Generating Input Files.....	33
3.9	Geometry Optimization.....	33
3.10	Single Point Energy Calculations	34
	CHAPTER 4 RESULTS AND DISCUSSION.....	35
4.1	Functional and Basis Set Determination	37
4.2	Acetophenones (C ₆ H ₅ COCH ₃).....	40
4.2.1	Geometrical Optimization	40
4.2.2	Atomic Charge	44
4.2.3	Spin Density	47
4.2.4	Frontier Molecular Orbitals.....	51
4.2.5	Muonium Hyperfine Interaction	54
4.3	2-fluoroacetophenone, 3-fluoroacetophenone, 4-fluoroacetophenone (FC ₆ H ₅ COCH ₃)	58
4.3.1	Geometrical Optimization	58
4.3.2	Atomic Charge	62
4.3.3	Spin Density	64
4.3.4	Frontier Molecular Orbitals.....	66

4.3.5	Muonium Hyperfine Interaction	68
4.4	2-chloroacetophenone, 3-chloroacetophenone, 4-chloroacetophenone (ClC ₆ H ₅ COCH ₃).....	74
4.4.1	Geometrical Optimization	74
4.4.2	Atomic Charge	76
4.4.3	Spin Density	79
4.4.4	Frontier Molecular Orbitals.....	80
4.4.5	Muonium Hyperfine Interaction	82
4.5	2-methylacetophenone, 3-methylacetophenone,4- methylacetophenone (CH ₃ C ₆ H ₅ COCH ₃)	86
4.5.1	Geometrical Optimization	86
4.5.2	Atomic Charge	89
4.5.3	Spin density	92
4.5.4	Frontier Molecular Orbitals.....	95
4.5.5	Muonium Hyperfine Interaction	96
CHAPTER 5 CONCLUSIONS AND RECOMMENDATIONS		102
5.1	Conclusions	102
5.2	Future Work	104
REFERENCES.....		105
APPENDICES		
LIST OF PRESENTATIONS		

LIST OF TABLES

		Page
Table 1.1	Structures of acetophenones used in this study.....	4
Table 2.1	The characteristic of the positive muon [24].....	7
Table 2.2	Mu hyperfine coupling constant in mono-substituted benzene, C ₆ H ₅ XTable.....	13
Table 4.1	The hyperfine field values of muoniated acetophenone from computational methods and experimental data.....	38
Table 4.2	The hyperfine field values of muoniated acetophenone by using different basis set.....	39
Table 4.3	Geometrical parameters of pure acetophenone and muoniated acetophenone at C6 (<i>ortho</i>).....	42
Table 4.4	Geometrical parameters of pure acetophenone and muoniated acetophenone at O13.....	43
Table 4.5	Atomic charge distributions of pure acetophenone and muoniated acetophenone at C6 (<i>ortho</i>).....	46
Table 4.6	Atomic charge distributions of pure acetophenone and muoniated acetophenone at O13.....	46
Table 4.7	Mulliken spin density of acetophenone for nearest neighbour atoms at Mu site that attached to C6 (<i>ortho</i>).....	47
Table 4.8	Mulliken spin density of acetophenone for nearest neighbour atoms at Mu site that attached to O13.....	48
Table 4.9	Relative energy and HFCC for calculated and experimental at seven Mu sites for acetophenone.....	56
Table 4.10	Geometrical parameters of pure 2-fluoroacetophenone and muoniated 2-fluoroacetophenone at O12.....	60
Table 4.11	Atomic charge distributions of pure 2-fluoroacetophenone and muoniated 2-fluoroacetophenone at O12.....	62
Table 4.12	Mulliken spin density of 2-fluoroacetophenone for nearest neighbour atoms at Mu site that attached to O12.....	65
Table 4.13	Relative energy and HFCC for calculated and experimental at six Mu sites for 2-fluoroacetophenone.....	69
Table 4.14	Relative energy and HFCC for calculated and experimental at six Mu sites for 3-fluoroacetophenone.....	71

Table 4.15	Relative energy and HFCC for calculated and experimental at six Mu sites for 4-fluoroacetophenone.....	72
Table 4.16	Geometrical parameters of pure 4-chloroacetophenone and muoniated 4-chloroacetophenone at C6 (<i>ortho</i>)	76
Table 4.17	Atomic charge distributions of pure 4-chloroacetophenone and muoniated 4-chloroacetophenone at C6 (<i>ortho</i>).....	77
Table 4.18	Mulliken spin density of 4-chloroacetophenone for nearest neighbour atoms at Mu site that attached to C6 (<i>ortho</i>).....	79
Table 4.19	Relative energy and HFCC for calculated and experimental at six Mu sites for 4-chloroacetophenone	83
Table 4.20	Relative energy and HFCC for calculated and experimental at six Mu sites for 2-chloroacetophenone	84
Table 4.21	Relative energy and HFCC for calculated and experimental at six Mu sites for 3-chloroacetophenone	85
Table 4.22	Geometrical parameters of pure 2-methylacetophenone and muoniated 2-methylacetophenone at C4 (<i>para</i>).....	88
Table 4.23	Geometrical parameters of pure 2-methylacetophenone and muoniated 2-methylacetophenone at O12.....	89
Table 4.24	Atomic charge distributions of pure 2-methylacetophenone and muoniated 2-methylacetophenone at C4 (<i>para</i>).....	89
Table 4.25	Atomic charge distributions of pure 2-methylacetophenone and muoniated 2-methylacetophenone at O12.....	90
Table 4.26	Mulliken spin density of 2-methylacetophenone for nearest neighbour atoms at Mu site that attached to C4 (<i>para</i>).....	93
Table 4.27	Mulliken spin density of 2-methylacetophenone for nearest neighbour atoms at Mu site that attached to O12.....	93
Table 4.28	Relative energy and HFCC for calculated and experimental at six Mu sites for 2-methylacetophenone	98
Table 4.29	Relative energy and HFCC for calculated and experimental at six Mu sites for 4-methylacetophenone	99
Table 4.30	Relative energy and HFCC for calculated and experimental at six Mu sites for 3-methylacetophenone	100

LIST OF FIGURES

	Page
Figure 2.1	The molecular structure of ketone..... 11
Figure 2.2	The structure of acetophenone 12
Figure 2.3	Structure of dicarbonyl substrate, cyclopent-4-ene1,3-dione I and its adduct radical formed (II , III and IV) [20]..... 14
Figure 2.4	TF-MuSR spectrum of radical formed by muonium atom addition to I at 299K (a) the low-frequency region corresponding to II and (b) at the much higher frequency corresponding to IV [20]..... 15
Figure 2.5	TF- μ SR spectra on a various monosubstituted <i>p</i> -acetophenone–Mu compound which are (a) 4-fluoroacetophenone, (b) 4-chloroacetophenone and (c) 4-methylacetophenone..... 16
Figure 3.1	Numbering scheme for monosubstituted acetophenone29
Figure 3.2	Geometry structure of the systems at the possible muonium sites.....31
Figure 4.1	The molecular structure of (a) pure acetophenone (b) muoniated acetophenone at C6 (<i>ortho</i>) and (c) muoniated acetophenone at O13 41
Figure 4.2	Atomic charge distribution for (a) pure acetophenone (b) muoniated acetophenone at C6 and (c) muoniated acetophenone at O13 45
Figure 4.3	Mulliken spin density of each atom in muoniated acetophenone at (a) C6 (<i>ortho</i>) and (b) O1349
Figure 4.4	Frontier molecular orbital energy levels diagram and the electronic distribution of the HOMO and LUMO for (a) pure acetophenone, (b) muoniated acetophenone at C6 and (c) muoniated acetophenone at O13 52
Figure 4.5	The molecular structure of (a) 2-fluoroacetophenone and (b) muoniated 2-fluoroacetophenone at O1259
Figure 4.6	Atomic charge distribution for (a) pure 2-fluoroacetophenone (b) muoniated 2-fluoroacetophenone at O12 63
Figure 4.7	Mulliken spin density of each atom in muoniated 2-fluoroacetophenone at O12 64

Figure 4.8	Frontier molecular orbital energy levels diagram and the electronic distribution of the HOMO and LUMO for (a) pure 2-fluoroacetophenone and (b) muoniated 2-fluoroacetophenone at O13	67
Figure 4.9	The molecular structure of (a) 4-chloroacetophenone and (b) muoniated 4-chloroacetophenone at C6 (<i>ortho</i>)	75
Figure 4.10	Atomic charge distribution for (a) pure 4-chloroacetophenone (b) muoniated 4-chloroacetophenone at C6	78
Figure 4.11	Mulliken spin density of each atom in muoniated 4-chloroacetophenone at C6 (<i>ortho</i>).....	80
Figure 4.12	Frontier molecular orbital energy levels diagram and the electronic distribution of the HOMO and LUMO for (a) pure 4-chloroacetophenone and (b) muoniated 4-chloroacetophenone at C6 (<i>ortho</i>).....	81
Figure 4.13	The molecular structure of (a) 2-methylacetophenone and (b) muoniated 2-methylacetophenone at C4 (<i>para</i>) and (c) muoniated 2-methylacetophenone at O12.....	87
Figure 4.14	Atomic charge distribution for (a) pure 2-methylacetophenone (b) muoniated 2-methylacetophenone at C4 and (c) muoniated 2-methylacetophenone at	91
Figure 4.15	Mulliken spin density of each atom in muoniated 2-methylacetophenone at (a) C4 (<i>para</i>) and (b) O12	94
Figure 4.16	Frontier molecular orbital energy levels diagram and the electronic distribution of the HOMO and LUMO for (a) pure 2-methylacetophenone, (b) muoniated 2-methylacetophenone at C4 (<i>para</i>) and (c) muoniated 2-methylacetophenone at O12	95

LIST OF SYMBOLS

Ψ	electronic wavefunction
Ψ_v^\uparrow	orbitals of α electrons
Ψ_v^\downarrow	orbital of β electrons
γ_e	electron gyromagnetic ratio
γ_μ	muon gyromagnetic ratio
μ^+	positive muon
π	pion
α_0	Bohr radius
e^+	positron
\hbar	Planck's constant
O	dipole operator
u	unpaired spin orbital
v	paired spin orbital
ν_e	neutrino
ν_μ	antineutrino
r	distance between the electron and muon
T_c	Critical temperature
$T_e(\vec{r})$	Kinetic energy of electron
$T_n(\vec{R})$	Kinetic energy of nuclei
V_{n-e}	potential energy between electrons and nuclei

LIST OF ABBREVIATIONS

μ SR	Muon spin rotation/resonance/relaxation
ALC	Avoided Level Crossing
AO	Atomic orbital
B3LYP	Becke, 3-Parameter , Lee, Yang and Parr
BO	Born-Oppenheimer
CCDC	Cambridge Crystallographic Data Centre
DFT	Density functional theory
ESR	Electron Spin Resonance
FMO	Frontier molecular orbital
GTO	Gaussian type orbital
HF	Hartree-Fock
HFCC	Hyperfine coupling constant
HOMO	Highest occupied molecular orbital
LCAO-MO	Linear combination of atomic orbital molecular orbital
LF	Longitudinal Field
LUMO	Lowest unoccupied molecular orbital
MPA	Mulliken Population Analysis
Mu	Muonium
NMR	Nuclear magnetic resonance
SCF	Self consistent field
STO	Slater type orbital
SVP	Split valence polarization
TF	Transverse Field
ZF	Zero Field

LIST OF APPENDICES

APPENDIX A	GEOMETRICAL STRUCTURE
APPENDIX B	ATOMIC CHARGE DISTRIBUTION
APPENDIX C	SPIN DENSITY
APPENDIX D	MOLECULAR ORBITAL ENERGY

KAJIAN PENGKOMPUTAN TERHADAP ASETOFENON TERMUONAT

ABSTRAK

Tesis ini melaporkan keputusan siasatan teori tapak hentian muonium yang (μ) ditambah dalam sistem asetofenon dengan penukar ganti (CH_3 , F, Cl) yang berbeza, serta interaksi hiperhalus pada muonium. Selain itu, kajian ini juga bertujuan untuk memahami struktur elektronik sistem termuonat. Kajian ini juga dapat memberikan pengetahuan yang lebih mendalam mengenai sifat-sifat struktur dan elektronik sistem sasaran dan dengan itu melengkapkan penemuan dari eksperimen *Muon Spin Rotation/ Relaxation/ Resonance* (μSR). Sepuluh sebatian terdiri daripada satu asetofenon tulen dan sembilan asetofenon yang digantikan dengan tiga penukar ganti yang berbeza (CH_3 , F, Cl) pada kedudukan *orto*, *meta*, *para*. Pengiraan Teori Ketumpatan Fungsian dilakukan menggunakan fungsi Becke, 3-Parameter, Lee, Yang dan Parr (B3LYP) ditambah dengan fungsi polarisasi dan fungsi resapan set asas 6-311++G(d,p), untuk melaksanakan pengoptimuman geometri untuk mendapatkan kedudukan μ yang paling stabil. Untuk setiap asetofenon yang termuonat dan asetofenon tertukar ganti, enam hingga tujuh tapak hentian μ berada di *orto*, *meta*, *para* pada gelang fenil dan pada kumpulan karbonil. Hasil yang dikira menunjukkan bahawa semua tapak hentian μ pada asetofenon dan asetofenon tertukar ganti didapati stabil. Kajian mengenai kepadatan putaran, pengagihan caj dan orbital molekul sistem termuonat menunjukkan ciri yang berbeza berbanding dengan sistem tulen. Nilai interaksi hiperhalus μ yang terperangkap di karbonil-O bagi semua sistem menunjukkan nilai gandingan terkecil yang bertepatan dengan nilai interaksi hiperhalus eksperimen dalam molekul dengan kumpulan karbonil. Secara amnya,

untuk cincin fenil, Mu di kedudukan *meta* memberikan nilai interaksi hiperhalus yang tertinggi. Interaksi hiperhalus yang terendah adalah pada kedudukan *ortho* di mana dijangkakan penarikan ketumpatan elektron yang paling besar, sementara kedudukan *para* berada di antara *ortho* dan *meta*. Kesimpulan ini melengkapkan penemuan eksperimen, dengan interaksi hiperhalus berada dalam urutan *meta* > *para* > *ortho* berkenaan dengan kedudukan kumpulan karbonil.

COMPUTATIONAL STUDIES ON MUONIATED ACETOPHENONES

ABSTRACT

This thesis reports the results of a theoretical investigation for the most possible location of muonium (Mu) implanted in sets of the acetophenone with different substituent (CH₃, F, Cl), as well as the corresponding Mu hyperfine interaction. Apart from that, this study aims at understanding the electronic structures of the muoniated systems. The study can also provide more fundamental knowledge on the structural and electronic properties of the targeted systems and thus complementing the findings from Muon spin rotation/resonance/relaxation (μ SR) experiments. Ten compounds that consist of one pure acetophenone and nine substituted acetophenones with three different substituents (CH₃, F, Cl) on the *ortho*, *meta*, *para* position. The Density Functional Theory calculation was carried out using the Becke, 3-Parameter, Lee, Yang and Parr (B3LYP) functional coupled with polarized and diffuse function basis set 6-311++G(d,p), to perform geometry optimization to get the most stable Mu position. For each of the muoniated acetophenone and substituted acetophenone, six to seven possible sites of Mu are considered which is at the *ortho*, *meta*, *para* on the phenyl ring and the carbonyl group. The calculated results showed that all the possible sites of Mu adducts on the acetophenone and substituted acetophenones were found to be energetically stable. The studies on spin densities, charge distribution and molecular orbitals of the muoniated systems showed a different characteristic compared to the pure systems. The hyperfine interaction value of Mu trapped at carbonyl-O for all the systems show the smallest coupling which is in agreement with the experimental hyperfine interaction values in molecules with carbonyl group. In general, for the

phenyl ring, μ at the *meta* site always gives the highest value of hyperfine interaction. The lowest hyperfine interaction is at *ortho* where the greatest withdrawal of electron density is to be expected, while the para position is in the midway between *ortho* and *meta* sites. This conclusion complements with the experimental findings, with the magnitude of the hyperfine interaction being in order $meta > para > ortho$ with respect to the position of the carbonyl group.

CHAPTER 1

INTRODUCTION

1.1 Research Background

In recent years, there are several μ SR (Muon spin rotation/resonance/relaxation) experiments and theoretical studies carried out on materials such as high-critical temperature (T_c) superconductors [1-5], organometallic compounds [1-6] and others including carbonyl group compounds [7-9]. The experimental investigations on carbonyl group, ketones, and aldehydes have been reported [9-11]. Most of the previous studies have focused on complex structures but there are lacks of studies on simple structures. The theoretical study on simple compounds such as muonium (Mu) adducts on phenyl ring substituted ketones such as acetophenone could be a good reference for future studies on more complex compounds.

The crystal structures of acetophenone determined by X-ray crystal analysis indicate a monoclinic crystal system with space group $P2_1/n$ [12]. However, only one theoretical investigation has been conducted on the muoniated system of acetophenone structures [9]. Most of the previous theoretical investigations related to the muon studies only focus on more complex structures such as zeolite [13], protein [13, 14], and tetraphenyl derivatives [15].

The studies of Mu adducts in materials had been carried out previously by using μ SR spectroscopic techniques [8-10, 16-18]. Muoniated radicals were confirmed by experimental studies. In these reports, an experimental study on ketones and phenyl ring substituted ketones and aldehydes was performed using transverse field muon spin

rotation (TF- μ SR) and longitudinal field muon spin relaxation (LF- μ SR) [8, 9]. It was found that there is a correlation between the hyperfine coupling constant of muonium and the vibrational frequency of the C=O bond of the ketone for those with phenyl group substituents, but not those with alkyl substituents [9]. According to the experimental studies, it was suggested that the muonium adds to a lone pair on the O and the unpaired electron ends up in the antibonding pi orbital. Therefore, it has resulted in half-breaking the pi-bond. Nevertheless, no computational investigations using the muon technique has been conducted to investigate these systems in detail. The results from the calculations would provide more detailed information which would help to elucidate the electronic structure including the population, and molecular orbital of the targeted systems. This research also aims to determine the most probable location of Mu stopping sites in mono-substituted acetophenones and to calculate the hyperfine coupling constant for Mu in these compounds.

1.2 Problem Statement

There are many μ SR studies of muonium addition in carbonyl group compounds [9-11, 16, 19, 20]. From the previous muonium experimental study, the results show that there is a correlation between the muonium hyperfine coupling constant (HFCC) and the vibrational frequency of the C=O bond. Additionally, there is also hyperfine interaction occur between the muonium with the carbon atom on the phenyl group where the muonium is attached at the *ortho*, *meta*, and *para* positions of the phenyl ring. However, the determination of the most probable location of muonium in some systems is not easy. This is because every experimental technique has its limitations and the same goes for the μ SR spectroscopic technique since it is unable to

determine the possible muonium site. The computational study can help to determine the most probable location(s) of the muonium in the host materials, complementing the experimental result. The study can also provide more fundamental knowledge on the structural and electronic properties of the target systems and thus complementing the findings from μ SR experiments.

1.3 Objectives

There are three objectives in this study as listed below:

1. To determine the most probable location of muonium stopping sites in mono-substituted acetophenones.
2. To study the electronic structures of these muoniated acetophenones.
3. To calculate the hyperfine coupling constants for Mu in the muoniated acetophenones.

1.4 Scope of Study

In this research, ten acetophenones are chosen as the host environment. Seven of the compounds have been reported in previous work which are acetophenone, 2-fluoroacetophenone, 3-fluoroacetophenone, 4-fluoroacetophenone, 4-chloroacetophenone, 2-methylacetophenone, and 4-methylacetophenone [8, 9]. The other three compounds are selected to expand the choices in order to include a correlation of the positions (*ortho*, *meta*, *para*) of the substituents at the phenyl rings.

The compounds are 2-chloroacetophenone, 3-chloroacetophenone and 3-methylacetophenone. The structures of the selected compounds are shown in Table 1.1.

Table 1.1 Structures of acetophenones used in this study

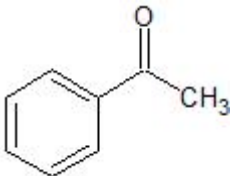
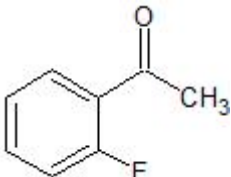
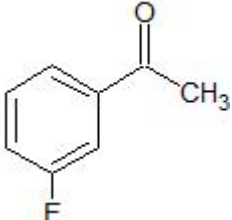
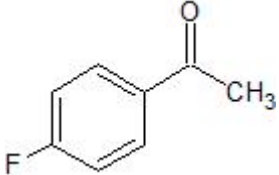
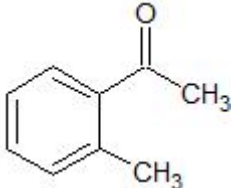
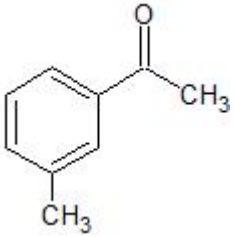
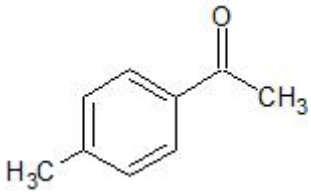
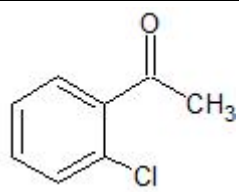
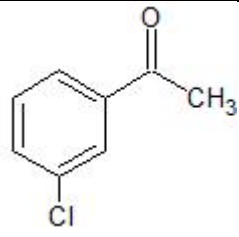
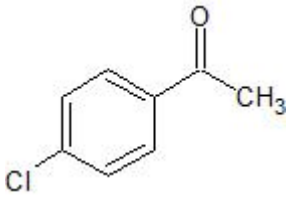
Compound Name	Structures
acetophenone	
2-fluoroacetophenone	
3-fluoroacetophenone	
4-fluoroacetophenone	
2-methylacetophenone	

Table 1.1 Continued

3-methylacetophenone	
4-methylacetophenone	
2-chloroacetophenone	
3-chloroacetophenone	
4-chloroacetophenone	

All the calculations were performed by using Gaussian09 software [21]. As for the visualising of the compounds and the results obtained from the calculations, GaussView5 [22] software is used. Linear Combination of Atomic Orbital - Molecular Orbital (LCAO-MO) calculations are employed in this project. The procedures will be discussed further in the subsequent chapter.

Calculations on the muonated system are crucial to be performed as they can verify the accuracy of the electronic structure. To verify the accuracy, it is necessary to obtain the information on the muon stopping sites. As the sites are confirmed, the hyperfine coupling constant calculated by the theoretical study will be compared with the hyperfine field examined by μ SR study. Therefore, the accuracy is proved to be acceptable if both results on the hyperfine interactions are in good accord.

CHAPTER 2

LITERATURE REVIEW

2.1 Muon and Muonium

The muon (μ^-) was discovered in 1937 by Neddermeyer and Anderson [23]. It is an elementary particle similar to the electron with a spin of 1/2. The muon antiparticle which is also known as an antimuon (μ^+) or positive muon, has a positive charge, a mass which is one-ninth the mass of the proton, and it is unstable, with the lifetime of 2.2 μs on average. Muons are produced by the decay of the short-lived positive or negative pions (π^\pm) as shown in Equation 2.1. The positive muon ultimately decays. The decay products are a positron (e^+), a neutrino (ν_e) and an antineutrino ($\bar{\nu}_\mu$), as shown in Equation 2.2. The properties of the positive muon are shown in Table 2.1.

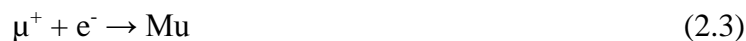
$$\pi^+ \rightarrow \mu^+ + \nu_\mu \quad (2.1)$$

$$\mu^+ \rightarrow e^+ + \nu_e + \bar{\nu}_\mu \quad (2.2)$$

Table 2.1 The characteristic of the positive muon [24]

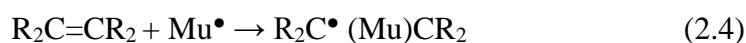
Properties	Values
Charge	(+e)
Spin	$\frac{1}{2}$
Mass	105.6595 MeV/c ² 0.1126096 m _p
Mean lifetime	2.19714 μs

When a positive muon enters the host material, it can capture an electron to form muonium, Equation 2.3. This is very similar to a proton picking up an electron to form a hydrogen atom since the positive muon in the matter may exist as a positive ion [25].



The muonium behaves chemically just like hydrogen, which can be considered as a second radioisotope of hydrogen after tritium [25]. This is because the ionization potential and Bohr radius of muonium are very close to a hydrogen atom. The difference between muonium and hydrogen is only in terms of mass, which is only one-ninth the mass of hydrogen.

The addition of muonium to an unsaturated bond in a molecular material results in the formation of muoniated radicals. The simplest example is indicated in Equation 2.4 [19].



Equation 2.4 shows that the addition of Mu in ethene results in the complete opening of the C=C double bond and forms C—Mu bond.

Muons are used in μSR to study the properties of materials because it can probe and provide microscopic information on its local environment. Thus, the studies would provide important information about the muoniated system such as the hyperfine interactions as well as the dynamics of the radical compounds produced.

2.2 Introduction to μ SR Techniques

μ SR is an excellent quantum beam based experimental technique that is mainly used in the field of condensed matter physics and material science involving muons where the muons are implanted in the materials. There are three distinct types of techniques, each utilizing the muon's asymmetric decay and its spin polarization [26], which are related by the acronym μ SR, consisting muon spin rotation, muon spin relaxation, and muon spin resonance [25, 26]. Muon spin rotation technique is an effective means of measuring magnetic field distribution [26, 27]. Muon spin relaxation technique is used to measure the fluctuating magnetic field while the muon spin in relaxation which means depolarization of muon spins [28]. Muon spin resonance is a variation of the more traditional magnetic resonance techniques like nuclear magnetic resonance (NMR) and electron spin resonance (ESR) [26].

The μ SR technique is applied by firing a beam of spin-polarized muons into the sample as a micro-magnetic probe to study the local magnetic field in various systems [24, 25]. As the muon is implanted and thermalized in the sample material, this technique is not considered a scattering technique. The muon interacts with the medium in many possible ways depending on its properties during the thermalization [26]. The unique properties of the pion and muon decay made the μ SR techniques possible. μ SR is a process in which a beam of spin-polarized muons is bombarded to a sample. The muons which are coming from pions are ensured to be 100% longitudinally-polarized with the spin opposite to their directions of motions. The muon spin will precess when the magnetic moment of muon interacts with local magnetic field and the spin polarization decrease [19]. Therefore, μ SR techniques could be excellent methods to investigate electronic and magnetic properties for

various states of matter. These techniques are very useful and practical compared to the other magnetic resonance probes such as NMR and ESR techniques that depend on thermal equilibrium spin polarization in the magnetic field [19, 29].

In Transverse Field Muon Spin Rotation (TF- μ SR), the polarized muon beam enters perpendicular to the magnetic field, and this technique is used to measure the hyperfine coupling constant of muon directly [30-32]. For the Longitudinal Field Muon Spin Relaxation (LF- μ SR), the applied external magnetic field is parallel to the initial direction of antimuon [30, 31]. The LF- μ SR technique is used to determine the activation energy value of the muoniated system. On the other hand, Zero Field Muon Spin Relaxation (ZF- μ SR) is yet another method to study materials without external magnetic field. Avoided Level Crossing (ALC- μ SR) is also another technique of μ SR. Similar to the LF- μ SR, this technique uses a magnetic field applied in a direction longitudinal to that of the muon beam [19].

The μ SR techniques have been reported in various studies [19]. This shows that it is a very practical and powerful tool to study muonium-substituted free-radicals in a variety of different environments [33].

2.3 Acetophenones

Ketones are simple organic compounds containing a carbonyl group (C=O) where the carbonyl group is attached to two hydrocarbon groups, R and R'. The formula of the ketone is RC(=O)R' as shown in Figure 2.1. These hydrocarbon groups can be either alkyl or aryl. The IUPAC system of nomenclature assigns a characteristic suffix of **-one** to ketones.

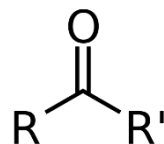


Figure 2.1 The molecular structure of ketone

The ketone carbon is sp^2 hybridized. It implements a trigonal planar geometry around the ketonic carbon in which the C–C–O and C–C–C bond angles are approximately 120 degrees [34]. The carbon-oxygen double bond in ketone is very highly polar because the oxygen is far more electronegative than the carbon. It has a strong tendency to pull electrons in carbon-oxygen bond towards itself. Ketone group can interact with other compounds through hydrogen bonding, and this capability of hydrogen bonding makes ketones more soluble in water than related methylene compounds. Ketones are not usually hydrogen bond donors, and they tend not to exhibit intermolecular attractions with other ketones [34]. Therefore, ketones are often more volatile than alcohols and carboxylic acids of comparable molecular weights.

Aromatic ketones are one of the categories of the ketones group. Aromatic ketones are compounds with a carbonyl attached on the aromatic structure to the other side of which one finds an alkyl or aryl group. The simplest example of an aromatic ketone is phenylethanone or also known as acetophenone. Acetophenone is the organic compound with the chemical formula C_8H_8O , and the structure is shown in Figure 2.2. It is a colourless, slightly oily liquid with a sweet, pungent orange blossom or jasmine-like odour [35].

Acetophenone is soluble in acetone, benzene, alcohol, chloroform, ether, fatty oils, and glycerol. It is also slightly soluble in water. Moreover, acetophenone also forms laminar crystals at low temperature and is flammable [35].

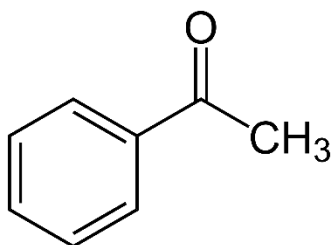


Figure 2.2 The structure of acetophenone

Acetophenone is used for fragrance in soaps and perfumes to impart an orange-blossom-like odour, and as a flavouring agent in foods. It is also used as the catalyst for the polymerization of olefins, which can act as a solvent for the synthesis of pharmaceuticals, rubber, chemicals, dyestuffs and corrosion inhibitors [35].

Acetophenone can be produced by many types of production methods, such as oxidation of ethylbenzene, catalytically from acetic and benzoic acids, from benzene and acetyl chloride in the presence of aluminium chloride, from benzene and acetic anhydride, the product from the oxidation of cumene, and by-product in the Hock phenol synthesis [35]. Besides, ketone and its derivatives have great fundamental importance in industries and various fields.

2.4 Related Studies on Muoniated Systems

The determination of the location of muon when it is trapped in the material is useful to interpret the local hyperfine field of the muon in the system [36]. There are several studies that have investigated the location of Mu for the systems containing a phenyl ring such as cyclohexadienyl, benzoic acid, benzene, styrene and acetophenone [9, 37-39]. The values of HFCC of Mu at three sites on phenyl ring which are *ortho*, *meta*, and *para* are obtained from the systems. The determinations of HFCC of the muoniated systems provide important information. The identification of HFCC value from the mono-substituted aromatic system has been reported to have different values [8, 9]. Table 2.2 lists the HFCC values of Mu on the three sites on the phenyl ring of mono-substituted benzene from the experimental results. The substituent X listed only indicate the substituent related to this study.

Table 2.2 Mu hyperfine coupling constant in mono-substituted benzene, C₆H₅X

X	Hyperfine coupling constant (A_μ) in MHz			Ref.
	<i>ortho</i>	<i>meta</i>	<i>para</i>	
H	514.6	514.6	514.6	[40]
CH ₃	489.6	509.3	496.4	[40]
F	485.7	511.8	511.8	[40]
Cl	487.3	509.4	485.3	[37]

The findings from the experimental studies reveal that Mu trapped in *meta* position for various aromatic systems give the highest value of Mu hyperfine coupling constant [8]. Roduner et al. reported that *meta* substitution has little effect on the hyperfine coupling constant because the molecular orbital with unpaired electron has a node in meta position [40]. The Mu HFCC for X=CH₃, F, Cl has been reported by

Roduner *et al.* [37, 40]. The studies show that the addition of Mu occurs preferentially in *meta*, followed by *para* and *ortho* respectively.

However, the aromatic system with the carbonyl group could have another Mu site on the carbonyl group [8, 9]. Further research on the systems containing the carbonyl group has been conducted. Rhodes *et al.* first observed a negative muon coupling constant in muonium–carbonyl adduct by using transverse-field muon spin rotation (TF- μ SR) technique [20]. Two radicals were detected in a dicarbonyl substrate, cyclopent-4-ene1,3-dione **I**; which are the desired carbonyl adduct **II**, and C=C adduct **IV**. Figure 2.3 shows a dicarbonyl substrate, cyclopent-4-ene1,3-dione structure and its adduct radicals formed. At temperature 299 K, the muon coupling measurement is 2.26 MHz for carbonyl adduct **II**, while C=C adduct **IV** of 384 MHz shown in Figure 2.4 [20].

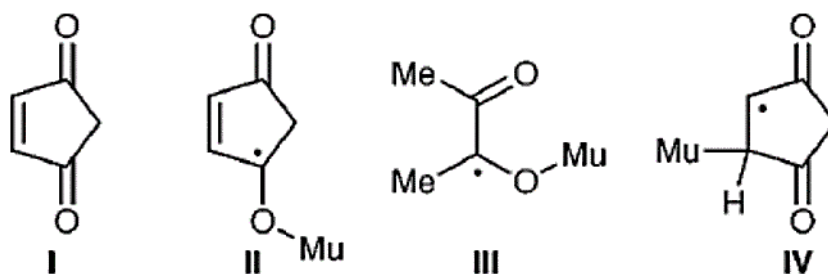


Figure 2.3 Structure of dicarbonyl substrate, cyclopent-4-ene1,3-dione **I** and its adduct radical formed (**II**, **III** and **IV**) [20]

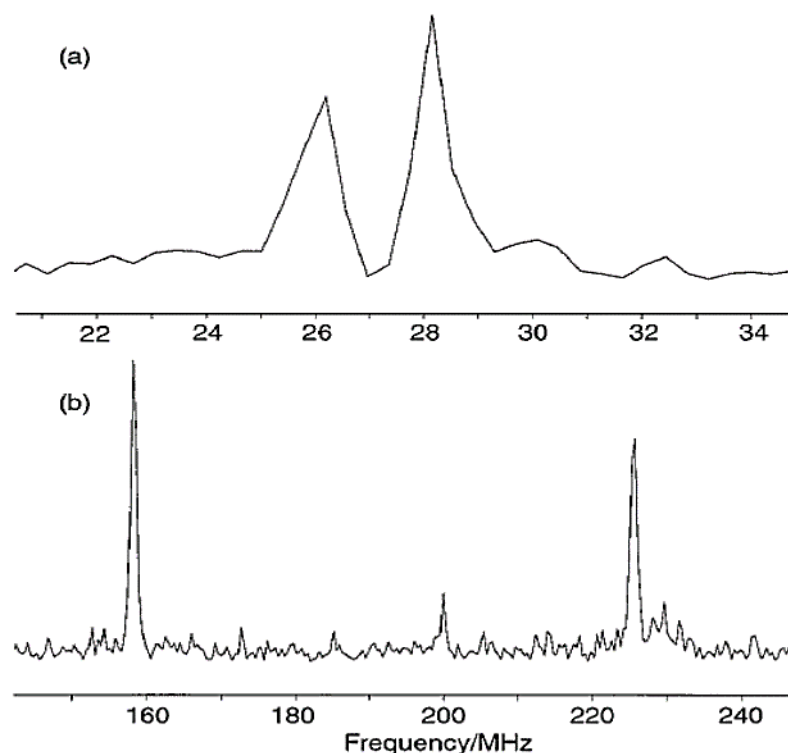


Figure 2.4 TF-MuSR spectrum of radical formed by muonium atom addition to **I** at 299K (a) the low-frequency region corresponding to **II** and (b) at the much higher frequency corresponding to **IV** [20]

Stride *et al.* performed TF- μ SR on a various monosubstituted *p*-acetophenone–Mu compounds which are 4-fluoroacetophenone, 4-chloroacetophenone and 4-methylacetophenone. In 4-fluoroacetophenone, three radical signals were observed with the muon coupling constant of 21.4 MHz, 485.5 MHz and 489.4 MHz [8, 9, 20]. Meanwhile, two radical signals of muon coupling constant were found in 4-chloroacetophenone which are 17.9 MHz and 481.0 MHz. While in 4-methylacetophenone, three radical species were detected which are 21.8 MHz, 476.6 MHz and 487.6 MHz [8, 9, 20]. Figure 2.5 shows the TF- μ SR spectra of various monosubstituted *p*- acetophenone–Mu compound. Stride *et al.* stated that the magnitudes of the hyperfine coupling constant being in order *meta* > *para* > *ortho* with respect to the position of the carbonyl group [8, 9, 20].

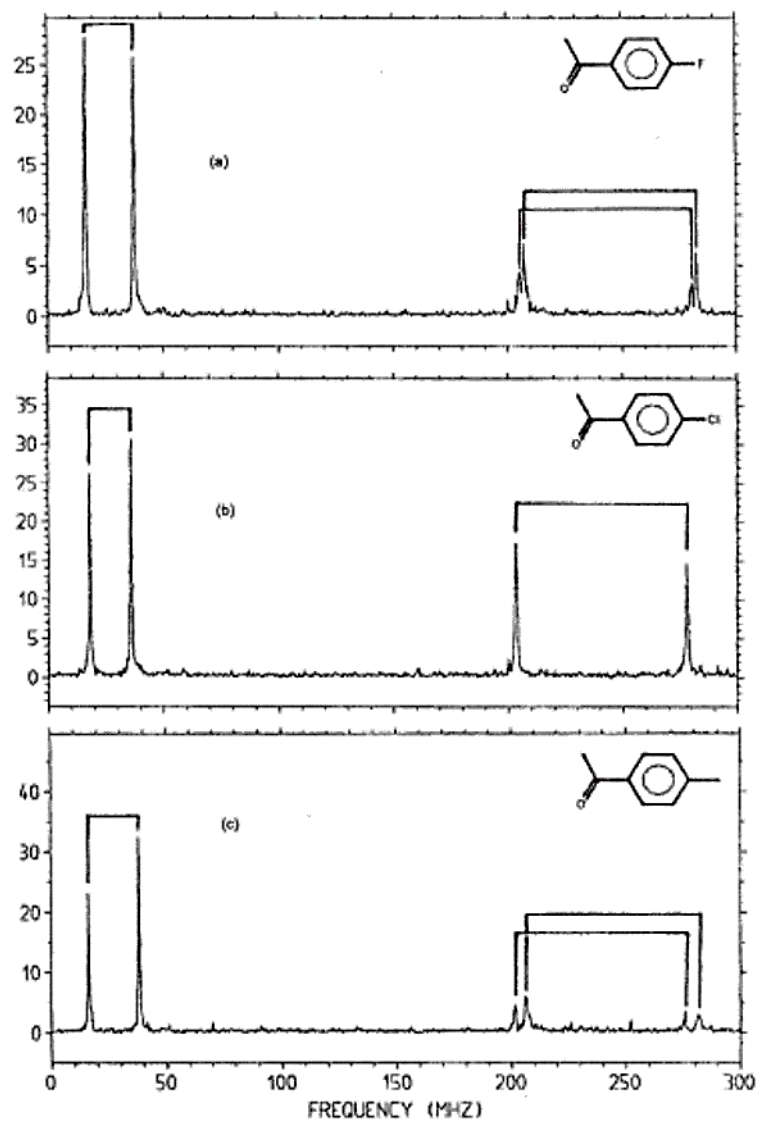


Figure 2.5 TF- μ SR spectra on a various monosubstituted *p*-acetophenone-Mu compound which are (a) 4-fluoroacetophenone, (b) 4-chloroacetophenone and (c) 4-methylacetophenone [8]

CHAPTER 3

METHODOLOGY

3.1 Computational Study

Computational chemistry is a part of chemistry that simulates chemical structures and reactions numerically, based on the fundamental of physics. It can be described as a study of the underlying chemistry using computers rather than chemicals. Due to the advances in computer development software and technological improvements in processing speed, the use of computational chemistry has grown rapidly. Today computational chemistry is an important complement to many experimental investigations in many chemistry fields as well as to atomic and molecular physics.

The quantum chemical calculations become a very useful method and are widely used to investigate materials such as large and complex compounds or compounds which are too costly to purchase or compounds that have yet to be synthesized. It also allows the scientists to investigate chemical phenomena by simulation using computers rather than complementary to examining compounds and reaction experimentally, calculations can be used both to make predictions before performing the actual experiments and to assist in the interpretation of the experimental results [41].

There are two parts in computational chemistry, which are molecular mechanics and electronic structure theory. Both of the areas perform the basic type of calculations such as computing the energy of a particular structure, performing

geometry optimizations and computing the vibrational frequencies of molecules resulting from interatomic motion within the molecule.

3.1.1 Molecular Mechanics

Molecular mechanics use a classical type models or the laws of classical physics approach to predict the energy and properties of the molecules such as predictions of equilibrium geometries and transition states, relative energies between conformers or between different molecules [42]. A simple algebra expression was used in molecular mechanics method in the expression of the total energy of the compound. This method does not include the wave function or total electron density in describing the total energy. The energy expression comprises of simple classical equations, for example, harmonic oscillator equation to explain the energy associated with bond stretching, bending, rotation and intermolecular forces, such as Van der Waals interactions and hydrogen bonding.

The molecular mechanics method has weaknesses and limitations. Although it is efficient to calculate large and complex compounds such as proteins and DNA, it is not capable enough to calculate the electronic properties of the system. Hence, to describe a system, a classical method is not a good approach.

3.1.2 Electronic Structure Methods

Electronic structure methods use the law of quantum mechanics, which is the basis for computational calculations. It is mainly concerned with the numerical computation of molecular electronic structure. The electronic structure methods can be classified into two major classes; the semi-empirical methods and *ab-initio* methods [42].

Semi-empirical methods use a simpler Hamiltonian than the correct molecular Hamiltonian and use parameters whose values are adjusted to fit the experimental data. In other words, they solve approximate parameters available for the type of chemical system in question. However, the *ab initio* methods are the correct molecular Hamiltonian [43]. They do not use experimental data except for the values of the fundamental physical constants. Moreover, it is a relatively successful approach to perform vibrational spectra.

3.2 *Ab initio* Methods

The term “*ab initio*” which comes from the Latin word which means “from the beginning” is one of the theoretical approaches that does not use empirical information. This method is based on quantum mechanics. Unlike molecular mechanics and semi-empirical methods, these methods calculate directly from quantum mechanics with no inclusion of experimental data [42].

This method is not limited to any specific class of system and the size of the system. In this quantum calculation, they converge to the exact solution and able to determine any type of atom including metal. *Ab initio* methods first optimize the

molecular geometry and then evaluate the second derivative at the equilibrium positions usually using analytical derivatives. They provide reliable values for harmonic vibrational frequencies for fairly large sized molecules. On the other hand, the calculations can be used to predict barriers to the internal rotation as well as relative stabilities of different conformers. The information obtained from structural parameters, conformational stabilities, force constants, vibrational frequencies as well as infrared and Raman band intensities give significant contributions to the field of vibrational spectroscopy. There are two principally different quantum mechanical approach addressing the vibrational problems. They are the Hartree-Fock (HF) method and the Density Functional Theory (DFT) method.

3.2.1 Hartree-Fock (HF)

The simplest type of *ab initio* method is HF. This method can be used for all types of molecules, and it can compute the structure of the system, vibrational frequency, including the transition state [44]. The HF method is very useful in solving the Schrödinger equation to approximate complex many-electron system. This method is merely based on electron and nuclei position which is very complicated to solve [45, 46]. However, the complexity can be reduced by applying the Born-Oppenheimer (BO) approximation. In this solution, only the interactions between the particles are approximated. This is due to the computational method which considered a motion of one electron to be independent of the dynamics of all other electrons [45]. Hartree-Fock is competent especially in determining the structures and vibrational frequencies of stable molecules and some other transition states. However, this theory has its weakness. It neglects the electron correlation and thus, makes it unsuitable for some

calculations. Using this method for the calculations is very time-consuming and demands high-performance computer. Hence, the computational cost for this method is expensive.

Therefore, there is an alternative to the *ab initio* method which is DFT. The DFT method has developed in the past several years as a successful alternative to traditional Hartree-Fock methods. The DFT methods, especially hybrid functional methods have emerged as a powerful quantum chemical tool in investigating the electronic structures in molecular systems [47-49].

3.2.2 Density Functional Theory (DFT)

Density functional theory (DFT) method is just the same as *ab initio* methods, but is much more computationally efficient in providing correlation energy [42, 49, 50]. In DFT calculations, the total energy calculated is represented in terms of the total electron density. Besides, this method is much less expensive especially regarding computer CPU time, memory and disk space.

In the framework of the DFT approach, different exchange and correlation functionals are routinely used. This method is widely employed because the electron correlation has been included in this method as an additional factor which reacts as a functional of the electron density. For hybrid DFT, the Becke-3-Lee-Yang-Parr (B3LYP) combination is the most used since it proved its capability in reproducing various molecular properties, including vibrational spectra, electronic transitions, nonlinear optical activity, NMR chemical shifts, molecular electrostatic potential [49]. The combination use of B3LYP functional and various standard basis sets would

provide an excellent compromise between accuracy and computational efficiency of the molecular properties, vibrational spectra, electronic transitions and others for more complex, large and medium size molecules.

3.3 Theoretical Background

3.3.1 The Schrödinger Equation

The Schrödinger equation plays the role of Newton's law and conservation of energy in classical mechanics. In quantum mechanics, the energetics and electronic structures of a molecular system are derived from the Schrödinger equation, subject to the appropriate boundary conditions [51]. The equation describes the wavefunction of particles:

$$\left\{ \frac{-\hbar^2}{8\pi^2m} \nabla^2 + V \right\} \Psi (\vec{r}, t) = \frac{i\hbar}{2\pi} \frac{\partial \Psi (\vec{r}, t)}{\partial t} \quad (3.1)$$

$$\nabla = \frac{\partial}{\partial x} \hat{i} + \frac{\partial}{\partial y} \hat{j} + \frac{\partial}{\partial z} \hat{k} \quad (3.2)$$

where,

Ψ is the wavefunction of the system

m is the mass of the particle

\hbar is Planck's constant

V is the potential field in which the particle is moving

The Schrödinger equation can be simplified using the mathematical technique called the separation of variables when V is not a function of time. When the wavefunction becomes the product of a spatial function and a time function:

$$\Psi(\vec{r}, t) = \Psi(\vec{r}) \tau(t) \quad (3.3)$$

Then when equation 3.3 is substituted into equation 3.1, it will produce two equations, which one of them is independent of time and the other one completely depends on time. In general, the time-independent Schrödinger equation is more familiar and will be focused entirely:

$$\hat{H}\Psi(\vec{r}) = E\Psi(\vec{r}) \quad (3.4)$$

$$\hat{H} = \frac{-\hbar^2}{8\pi^2m} \nabla^2 + V \quad (3.5)$$

Where E is the total energy of the particle, and \hat{H} is the Hamiltonian operator. Equation 3.4 can produce a variety of solutions depending on the stationary states of the particle. However, it does not provide an accurate description of the core electrons in large nuclei.

3.3.2 The Born-Oppenheimer Approximation

The approach is named after Max Born and J. Robert Oppenheimer. Born-Oppenheimer (BO) approximation is used to simplify the solution of the Schrödinger equation [51]. The full Hamiltonian for the molecular system is written as below:

$$\mathbf{H} = \mathbf{T}_e(\vec{r}) + \mathbf{T}_n(\vec{\mathbf{R}}) + \mathbf{V}_{n-e}(\vec{\mathbf{R}}, \vec{r}) + \mathbf{V}_e(\vec{r}) + \mathbf{V}_n(\vec{\mathbf{R}}) \quad (3.6)$$

This approximation consists of two parts; the electronic and nuclear motions. In the first part of the BO approximation, it is used to simplify the electronic Hamiltonian equation. The electronic Hamiltonian equation is given by:

$$\mathbf{H}_e\Psi_e(\vec{r}, \vec{\mathbf{R}}) = E_{\text{eff}}(\vec{\mathbf{R}})\Psi_e(\vec{r}, \vec{\mathbf{R}}) \quad (3.7)$$

The effective nuclear potential function, E^{eff} can be obtained by solving the equation 3.7. E^{eff} is also used as the effective potential for the nuclear Hamiltonian:

$$\mathbf{H}_n = \mathbf{T}_n(\vec{\mathbf{R}}) + E_{\text{eff}}(\vec{\mathbf{R}}) \quad (3.8)$$

Equation 3.8 is used in the Schrödinger equation for a nuclear motion to describe the vibrational, rotational, and transitional states of the nuclei.

3.4 Muonium Hyperfine Interaction

Hyperfine interaction is the interaction between the magnetic moment of a nucleus and its surrounding spin [52]. The hyperfine interactions are very sensitive to the local electronic structure near the nuclei where the interactions occur. The interactions are very small compared to the energy levels of the nucleus itself. The hyperfine interaction can be divided into two parts. The first part is the Fermi contact interaction or the isotropic and the second type is the dipolar interaction or anisotropic. Fermi contact occurs only with the s electrons, while dipolar interaction is due to electrons in the p and d orbitals [52]. The isotropic hyperfine coupling constant of Mu, A and the Mu anisotropic hyperfine coupling constant, B can be calculated using the following formula[52].

$$A = \frac{4}{3} \gamma_e \gamma_\mu \hbar (10^{-6} a_0^{-3}) [|\Psi_u^\uparrow(\mathbf{R})|^2 + \sum_v \{ |\Psi_v^\uparrow(\mathbf{R})|^2 - |\Psi_v^\downarrow(\mathbf{R})|^2 \}] \quad (3.9)$$

$$B = \frac{1}{4\pi} \gamma_e \gamma_n \hbar (10^{-6} a_0^{-3}) \left[\sum_v \{ \langle \Psi_v^\uparrow | \mathbf{O} | \Psi_v^\uparrow \rangle - \langle \Psi_v^\downarrow | \mathbf{O} | \Psi_v^\downarrow \rangle \} + \langle \Psi_u^\uparrow | \mathbf{O} | \Psi_u^\uparrow \rangle \right] \quad (3.10)$$